

Unusual Island Formations of Ir on Ge(111) Studied by STM

M. van Zijll, E. Huffman,¹ D. Lovinger,² and S. Chiang

Department of Physics
University of California Davis
1 Shields Ave.
Davis, CA 95616-5270 USA

Abstract

Island formation on the Ir/Ge(111) surface is studied using ultrahigh vacuum scanning tunneling microscopy. Ir was deposited at room temperature onto a Ge(111) substrate with coverages between 0.5 and 2.0 monolayers (ML). The samples were annealed to temperatures between 550 and 800 K, and then cooled prior to imaging. With 1.0 ML Ir coverage, at annealing temperatures 650-750 K, round islands form at locations where domain boundaries of the substrate reconstruction intersect. Both the substrate and the islands display a $(\sqrt{3} \times \sqrt{3})R30^\circ$ reconstruction. Additionally, a novel surface formation is observed where the Ir gathers along the antiphase domain boundaries between competing surface domains of the Ge surface reconstruction. This gives the appearance of the Ir in the domain boundaries forming pathways between different islands. The islands formed at higher annealing temperatures resulted in larger island sizes, which is evidence of Ostwald ripening. We present a model for the islands and the pathways which is consistent with our observations.

Keywords: STM; island formation; surface dislocations; metal-semiconductor interface; iridium; germanium

¹ Present address: Department of Physics, Duke University, Durham, NC 27708, USA

² Present address: Department of Physics, University of California San Diego, La Jolla, CA 92093, USA.

© <2017>. This manuscript version is made available under the CC-BY-NC-ND 4.0 license <http://creativecommons.org/licenses/by-nc-nd/4.0/>

1. Introduction

The restructuring of semiconductor surfaces, upon adsorption of metals, is of fundamental interest in surface physics. A practical application is the fabrication of electronic devices. Our group has done much work recently on studying and characterizing different low-index single crystal surfaces of clean Ge [1]. We have also studied the surface characteristics arising from the evaporation of different metals onto a Ge substrate.[2-8]

In addition to Frank-Van der Merwe (layer-by-layer), Volmer-Weber (three-dimensional (3D) islands), and Stranski-Krastanov (layer plus islands) growth,[9] other interesting growth modes are sometimes observed, such as 1D growth (islands with high aspect ratios in preferred directions) [5, 10]. The growth type depends on the combination of the metal and semiconductor chosen, the Miller indices of the substrate, and the dosing and annealing temperatures. The sizes of the islands generally increase with higher annealing temperatures for cases which can be described by Ostwald ripening.[11] The local geometry of the surface, such as the existence of steps or defects, also has a clear role in the types of islands formed.

Ir surface structures have been studied relatively little despite the many interesting metals located nearby on the periodic table [12-14]. For this paper, we studied Ir/Ge(111) with Ir coverage between 0.5 and 2.0 monolayers (ML), and annealing temperatures between 550 and 800 K. With 1.0 ML Ir coverage, at annealing temperatures 650-750 K, round islands form at locations where domain boundaries intersect. Both the substrate and the islands display a $(\sqrt{3} \times \sqrt{3})R30^\circ$ (hereafter referred to simply as $\sqrt{3}$) reconstruction. Additionally, a novel surface formation is observed where the Ir gathers along the antiphase domain boundaries between competing surface domains of the Ge surface reconstruction. This gives the appearance of the Ir in the domain boundaries forming pathways between different islands.

2. Experimental details

The instrumentation we use is the first apparatus that combined a low energy electron microscope (LEEM) [15, 16], X-ray photoemission spectrometer (XPS), and a scanning tunneling microscope (STM), [17] into a common ultrahigh vacuum (UHV) system [18] with a base pressure of 2×10^{-10} torr. Using a modified sample holder which is compatible with all three instruments, an identical sample can be observed using LEEM, XPS, and STM without breaking vacuum.

Ge(111) samples were placed into UHV, where the samples were sputtered using Ar^+ ions with 250 eV energy and $\sim 4 \mu\text{A}$ sputtering current. Subsequently, they were annealed at $\sim 800^\circ\text{C}$ until they were clean and displayed the $c(2 \times 8)$ surface reconstruction as viewed by STM [19, 20]. A clean Ge sample was used for each annealing experiment.

The Ge(111) samples were dosed with monolayer (ML) and sub-monolayer coverages of Ir and then annealed to a temperature between 550 K and 800 K in the STM. The samples were heated by resistive heating of a filament located near the sample; a thermocouple attached to the sample allowed measurement of the temperature. The samples were heated at a constant rate, and it took between 8 and 15 minutes to heat the sample to the target temperature with the longer times corresponding to higher temperatures. The sample was held at the final annealing temperature for 5 minutes. The sample was cooled in UHV conditions and imaged at either 400 K or room temperature (RT). After the sample cooled, it was imaged using STM. Because the samples were only annealed for 5 minutes, it is likely that longer annealing times would produce some observations similar to higher annealing temperatures. Data were analyzed and plotted using WSXM [21].

The dosing rate of the Ir evaporator was determined by comparing experimental XPS spectra[8] to simulated spectra computed using SESSA.[22]. The Ir coverage for completion of an observed $\sqrt{3}$ overlayer in LEEM was determined to be ~ 2.0 ML.[8] With the assumption that the deposition rate maintained a constant flux, this calibration was used for the STM data presented in this paper.

3. Results and discussion

3.1. Observations of Ir features as a function of coverage

STM images of Ge samples with 0.5, 1.0, and 2.0 ML Ir coverage are shown in Figs. 1(a)-(c). For 0.5 ML, small round islands are seen which appear tall compared to the substrate. For 1.0 ML, round islands are observed which are larger and cover a greater surface area, compared to the sample with 0.5 ML. Even though a complete ML of Ir is deposited in Fig. 1(b), the islands cover about half of the surface. Figure 1(b) also shows two step edges of the Ge substrate. Figure 1(c) shows 2.0 ML Ir coverage, for which a nearly-complete over layer of Ir is formed. Vacancy islands form at locations where the overlayer is not complete; two of the vacancy islands are outlined in Fig. 1(c). The overlayer observed in Fig. 1(c) correlates with the coverage at which a completed overlayer was observed in LEEM images.[8]

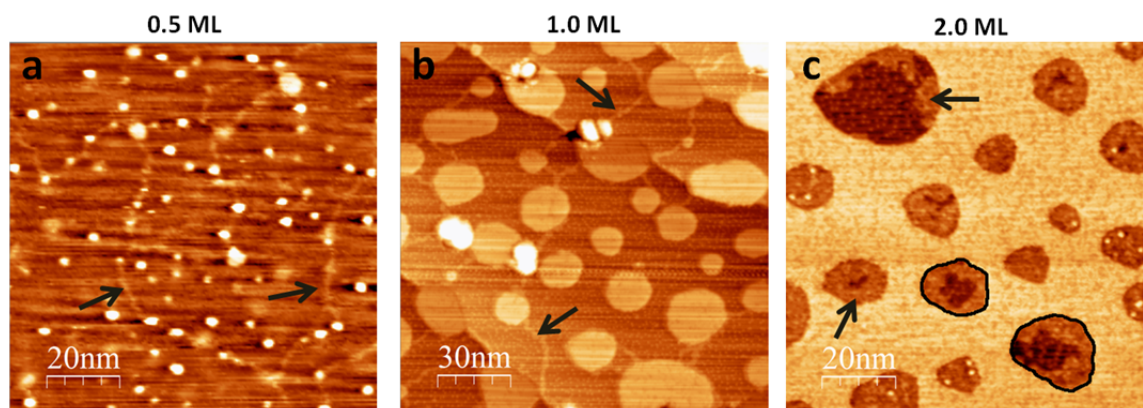


Figure 1: STM topographic images showing different coverages of Ir on Ge(111) which were annealed to similar temperatures, and then cooled to RT for imaging. (a) 0.5 ML, 750K. (b) 1.0 ML, 700K. (c) 2.0 ML, 700K. Two of the vacancy islands are outlined in (c). Arrows in (a)-(c) point to features of an intermediate height between the Ge substrate and the islands in (a)-(b) or the overlayer in (c). Sample bias was -2.0 V for each image. Tunneling current was 2 nA.

The arrows in Figs. 1(a) and 1(b) point to features which appear at an intermediate height between the Ge substrate and the islands. These features typically appear as thin lines connecting different islands. We call these features pathways. The arrows in Fig. 1(c) point to intermediate features located inside the vacancy islands next to the perimeter. Similar to the features indicated by arrows in Figs. 1(a) and (b), the features in Fig. 1(c) appear at an intermediate height between the Ge substrate and the overlayer; in contrast, however, these features have lower aspect ratios and cover a larger surface area. Many vacancy islands in Fig. 1(c) are completely filled with this feature. As discussed in Sect. 3.2, we suspect that both the islands and the intermediate features, such as pathways, are primarily composed of Ir.

Figures 2(a) and 2(b) show magnified images of different regions of Fig. 1(b), and Fig. 2(c) shows a magnified image of a region of 1(c). The arrows in Fig. 2(a) show the location of a Ge step edge. Pathways are often found along upper step edges (middle arrow) except for locations where islands border the step-edge on the lower step (upper and lower arrow). The islands seen along the lower step-edge often protrude into the upper step-edge. The model we present for the islands in section 3.5 includes 1.0 ML of Ge as part of the island structure. The protrusion of the islands into the step edge may be due to the abundance of Ge available to diffuse from the step edge. The absence of pathways along the upper step edge at these locations may similarly be due to the diffusion of Ir into the island structure.

The arrows in Figs. 2(b) and (c) point to small features which become apparent with

higher magnification; we call these dots. The appearance of dots in both Figs. 2(b) and (c) indicates that the corresponding surfaces are similar. The dots appear dispersed on the substrate without long-range order.

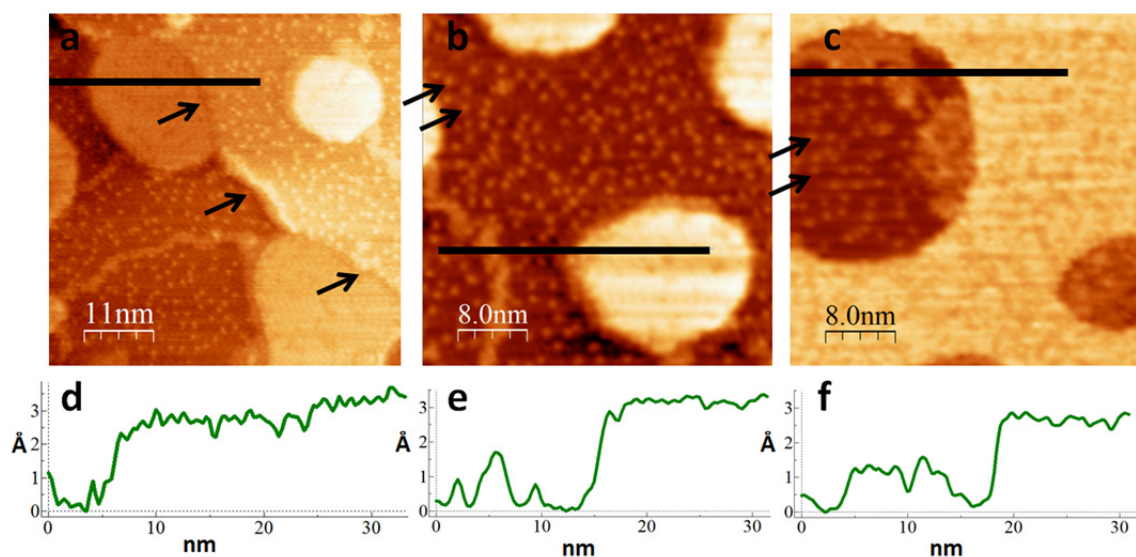


Figure 2. (a) and (b) Magnified images of different regions of Fig. 1(b). (c) Magnified image of a region of Fig. 1(c). Line profiles (d)-(f) are taken along the lines in the figures above them. The arrows in (a) indicate a step-edge. The arrows in (b) and (c) indicate dot features. Sample bias was -2.0 V for each image. Tunneling current was 2 nA.

that the height of the island appears slightly lower than the height of the Ge step edge; the surfaces are easily distinguished in Fig. 2(a) because dots only appear on the substrate. The line profiles in Figs. 2(e) and 2(f) show that the height of the island (b) is similar to the height of the overlayer (c). Since the overlayer corresponds to 2.0 ML Ir coverage, the round islands likely correspond to 2.0 ML Ir. The line profiles (e) and (f) also show the apparent heights of some intermediate features. The pathways are similar in height to the intermediate features inside the perimeter of the vacancy islands. The dots appear slightly lower than the other intermediate features. The difference in apparent height between the intermediate features and the tall features

may be attributed either to a change in the surface composition, or to a change in physical height, or both.

3.2. High resolution STM image: chemical effects and $\sqrt{3}$ reconstruction

Figure 3 shows an STM image of 1.0 ML Ir on Ge(111) which was annealed to 700 K. Although the tip bias was held constant during the acquisition, the resulting image shows surface features appearing differently in the three sections labeled I, II, and III. The borders between different sections run horizontally across the image, suggesting that a change in the tunneling tip must have occurred. Presumably, the addition or removal of a contaminant could cause a change in the work function, as well as the form of the local density of states of the tip for different regions of the image.

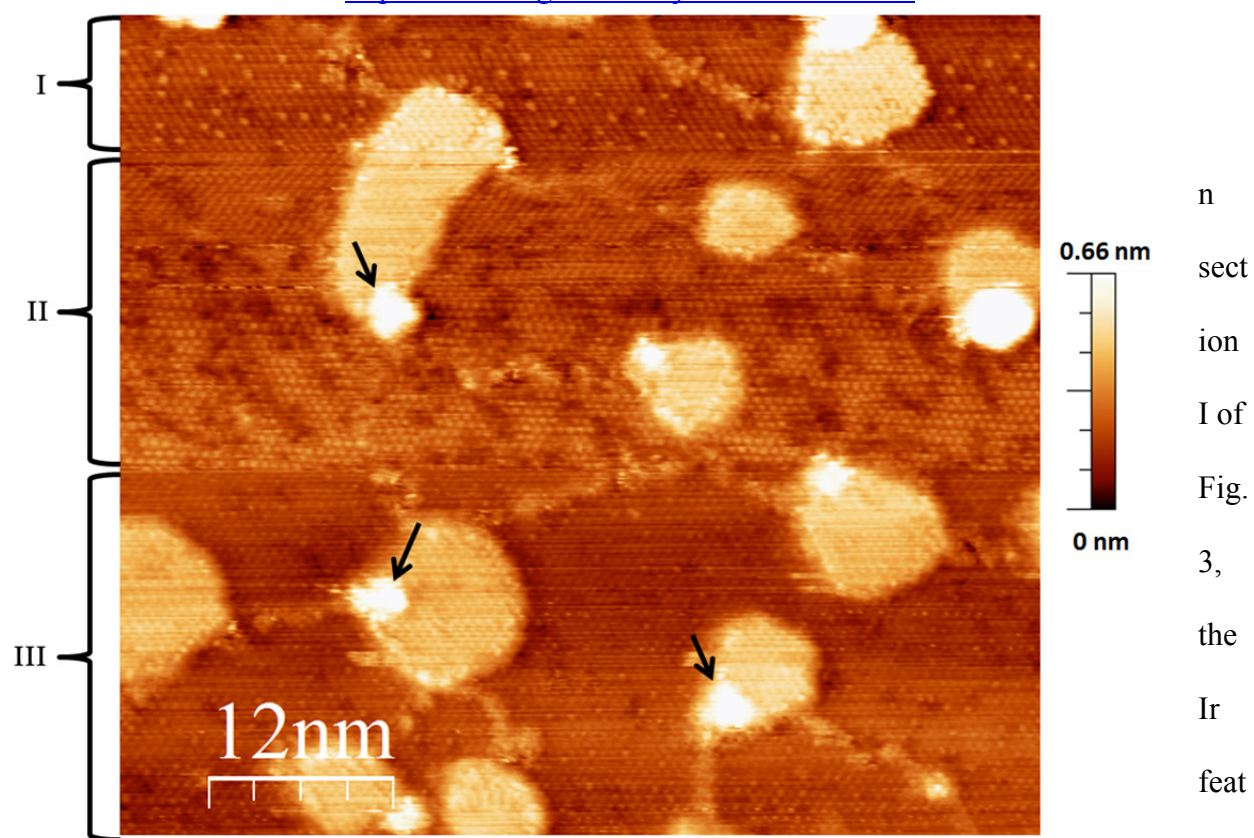


Figure 3. STM topographic image of 1.0 ML Ir on Ge(111), dosed at RT, annealed to 700 K, then cooled to RT for imaging. The state of the tip changed multiple times during this image, resulting in three unique surface appearances, indicated by sections labeled I, II, and III. The arrows indicate mounds. Note that Figures 4 and 5 are magnified images of regions of this figure. Sample bias was -2.0 V. Tunneling current was 2 nA.

with respect to the Ge substrate, with distinct dots, pathways, and islands evident. In section II, typical pathways and dots are not clearly distinguishable. In section III, the pathways are clearly seen but the dots are not evident. The height of the round islands in section I measures $2.6 \pm 0.1 \text{ \AA}$ above the substrate reconstruction, while round islands in sections II and III measure $2.0 \pm 0.1 \text{ \AA}$ and $2.2 \pm 0.1 \text{ \AA}$, respectively. The height of the pathways depends on the tip state in a similar manner to the islands; pathways were typically about $1.5 \pm 0.3 \text{ \AA}$ lower than the height of comparable islands.

It is likely that similar surface features (round islands, dots, and pathways) are present in

all three sections of Fig. 3, but tip contamination makes the features appear differently in each section. Section II shows a large number of negative features on the substrate. Some of these negative features can be attributed to substrate vacancies which are seen in all sections of Fig. 3. Other negative features in section II likely correspond to dots which appear positive in section I. In section I, a dot appears as a positive protrusion similar in size to a single Ge atom. In section II, a dot may appear as a negative protrusion with an apparent effect on the local density of states (LDOS) over a larger surface area.

Additional features in Fig. 3, which we call mounds, are indicated by arrows. Mounds are tall features which are typically located near the edge of an island. In Fig. 3, the heights of the mounds range from 2 to 6 Å above the island height. These mounds are evidence that these surface structures can exhibit some 3D growth.

Figure 4, a magnified image of a region of Fig. 3, shows a $\sqrt{3}$ reconstruction of the surface. This correlates with the $\sqrt{3}$ LEED pattern observed for similar annealing temperatures.[8] The $\sqrt{3}$ features on the substrate have two different types of appearances: (1) the brighter dots and (2) the bumps that appear across most of the surface, such as those indicated by the three neighboring black arrows with $\sqrt{3}$ spacing in Fig. 4(a). In the different regions of Fig. 3, the dots change height with respect to the bumps in a similar manner to the pathways and the islands, making it likely that the dots, pathways, and islands all correspond to Ir features. The bumps, on the other hand, have different chemical character and are likely to be either reconstructed Ge adatoms of the substrate or IrGe alloy. While the $\sqrt{3}$ reconstruction is commonly observed following metal deposition of Ge or Si and annealing [12, 14, 23-25], it has also been seen on the clean surfaces of Ge and Si prior to the formation of the typical $c(2\times 8)$ or

7x7 reconstructions [23, 26, 27]. Therefore, we think it is more likely that the bumps correspond to single Ge adatoms.

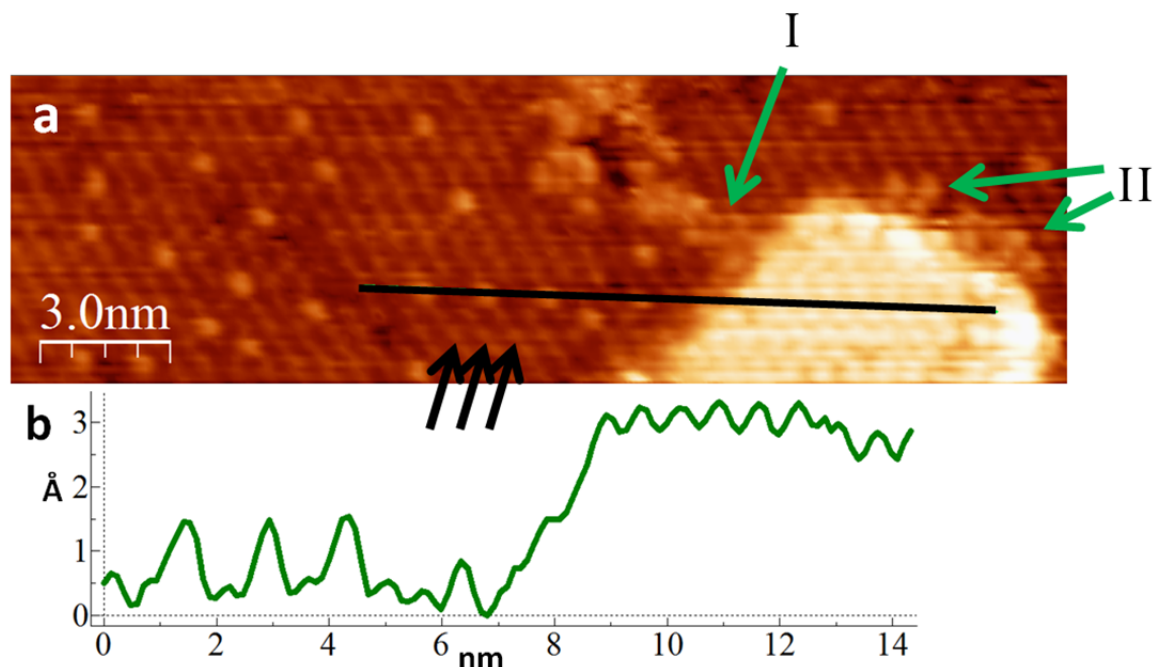


Figure 4. (a) STM topographic image of 1.0 ML Ir on Ge(111), dosed at RT, annealed to 700 K, then cooled to RT for imaging. (b) Line profile taken along the line in (a). The three neighboring black arrows point to features with $\sqrt{3}$ spacing. The arrow labeled I indicates a pathway segment. The arrows labeled II indicate intermediate features along the border of the island. Sample bias was -2.0 V. Tunneling current was 2 nA.

The $\sqrt{3}$ reconstruction is present on both the substrate and the islands. If each unit cell in the $\sqrt{3}$ reconstruction of the islands had one atom, this would represent a local coverage of 0.33 ML. Since the islands have 2.0 ML Ir coverage, the unit cell must consist of six Ir atoms. Based on the typical atomic radius of Ir, these atoms could not all fit in a single layer. Therefore, we infer that the islands consist of more than one physical layer of Ir. A model is presented in section 3.5.

The intermediate dot features in Fig. 4(a) appear to fall directly on top of the Ge adatoms. Pathways are composed of protrusions similar in appearance to dots. A segment of a pathway in

Fig. 4(a) is labeled I. The protrusions that make up a pathway have $\sqrt{3}$ spacing in some locations, but in other locations, they are more closely packed. Pathways often display defects, such as the one located to the left of I in Fig. 4(a).

Intermediate-sized protrusions similar to those that compose the pathways and dots are often seen around the entire perimeter of round islands; examples in Fig. 4(a) are labeled II. The location of these intermediate features directly next to the 2.0 ML islands is similar to the location of intermediate features in Fig. 1(c), which were seen inside vacancy islands directly next to the 2.0 ML overlayer. Since we have concluded that the Ir atoms composing the islands cannot fit in a single layer, these images suggest that the pathways, and intermediate features surrounding the islands, may simply be composed of fewer layers than the islands.

3.3. Pathway formation along dislocations of the reconstructed substrate

Figure 5 shows an analysis of the $\sqrt{3}$ surface domains near pathways. The contrast in this image is adjusted to accentuate the substrate features, causing the round island and the two pathways to appear over-saturated. The lines labeled I and II in Fig. 5 are guidelines, each of which crosses over a pathway. For I, the guideline falls between rows of adatoms on the left side of the pathway, and it directly overlaps rows of adatoms on the right side. Similarly, for II, below the pathway the guideline falls between rows of adatoms, and it directly overlaps rows of adatoms above. We thus conclude that the pathways perfectly follow the antiphase domain boundaries between competing surface domains of the Ge $\sqrt{3}$ surface reconstruction [28].

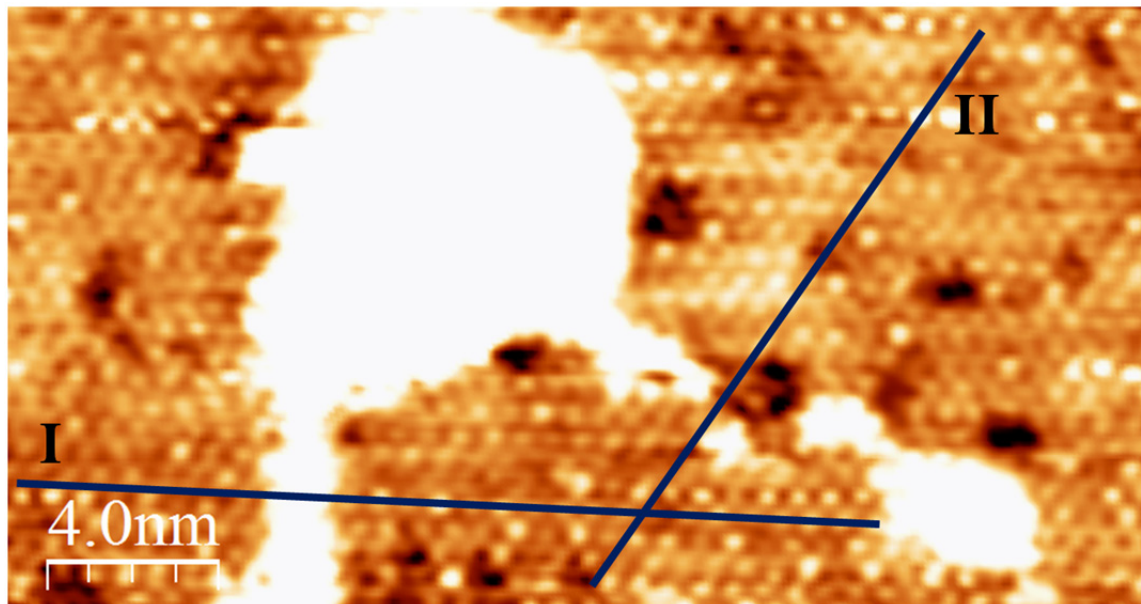


Figure 5. STM topographic image of 1.0 ML Ir on Ge(111), dosed at RT, annealed to 700 K, and then cooled to RT for imaging. The contrast in this image is adjusted to accentuate the substrate features, saturating the brightness of the round island and the two pathways. The guidelines show the domains on opposite sides of the pathways are different; on one side of a pathway the guidelines directly overlap rows of adatoms, and on the other side of a pathway they fall between rows. Sample bias was -2.0 V. Tunneling current was 2 nA.

The formation of pathways at domain boundaries suggests that Ir prefers to bind to sites with different chemical character than the $\sqrt{3}$ Ge adatom reconstruction; that these sites are adjacent at the domain boundary leads to the formation of contiguous Ir structures. We note that step-edges would also have different chemical binding for Ir atoms than the $\sqrt{3}$ reconstruction. This is completely consistent with the observation of pathways at step edges that was shown in Fig. 2(a). This trend is further supported by the locations of round islands, which typically form at locations where multiple pathways converge, i.e., where domain boundaries intersect. In contrast, the dots, which appear at locations of $\sqrt{3}$ coverage of Ge adatoms, are rarely seen neighboring one another when not bordering pathways or islands.

3.4. Annealing causes changes in Ir island formations

STM images of samples with 1.0 ML Ir coverage that were prepared with different final annealing temperatures are shown in Fig. 6. Figures 6(a) and 6(b) show the surface at low annealing temperatures for which the deposition of Ir is evenly spread across the surface. Notice that the scale bar for 6(a) and (b) has half the range of those in 6(c)-(f). Figure 6(c) shows distinct, tall, island formation with interconnected wormy shapes; the corresponding annealing temperature of 600 K is the lowest for which distinct island formation was observed. As the annealing temperature is increased from 600 to 640 K, the islands become less interconnected and rounder. This temperature range also corresponds to the formation of the $\sqrt{3}$ surface reconstruction observed with LEED for samples annealed to temperatures above 623 K.[8] Figure 6(d) shows islands which have a rounder shape compared to Fig. 6(c). Figures 6(e) shows the formation of typical islands and skinny pathways for 700 K annealing temperature, as already shown in Figs. 3-5 and discussed above. Figure 6(f) shows evidence of Ostwald ripening for the annealing temperature of 800 K. The bright mounds in Fig. 6(f) are 2-5 nm in height.

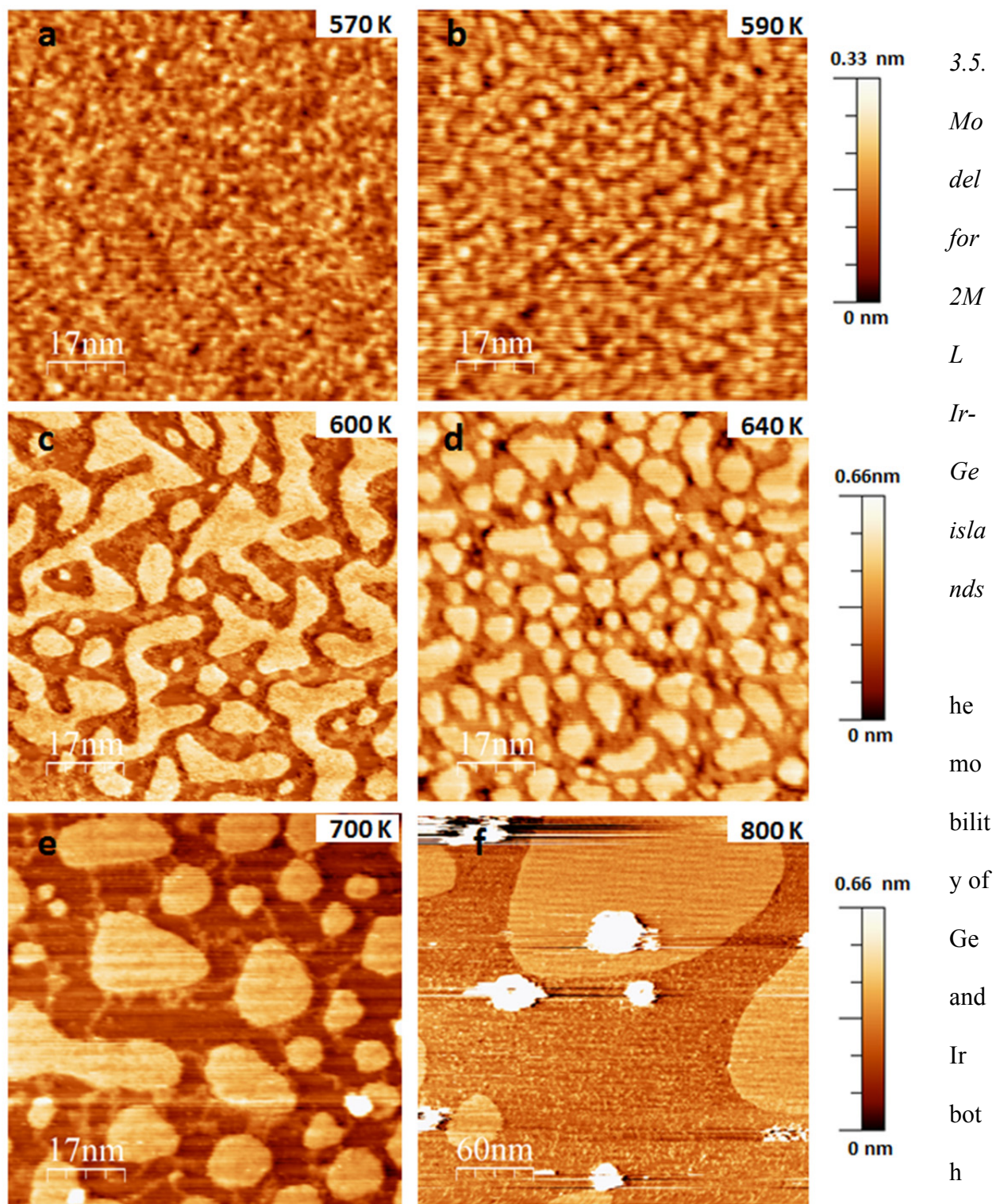


Figure 6: STM topographic images showing 1.0 ML Ir on Ge(111) annealed to (a) 570 K, (b) 590 K, (c) 600 K, (d) 640 K, (e) 700 K, (f) 800 K, and then cooled to RT for imaging. The vertical scale bars are associated with the row of images next to which they appear. Sample bias was -2.0 V for all images. Tunneling current was 2 nA.

© <2017>. This manuscript version is made available under the CC-BY-NC-ND 4.0 license <http://creativecommons.org/licenses/by-nc-nd/4.0/>

with annealing temperature. The sudden increase in height of surface features at 600 K (Fig. 6(c)) may suggest that Ge is diffusing into the islands [25, 29]. Domain boundaries, which are the locations of pathways and islands, also correspond to locations of the highest Ge diffusion rate during annealing [30]. Therefore, we present a model for the 2.0 ML Ir islands in Fig. 7 that involves both Ir and Ge atoms, but it is only one of many possibilities. We assume most of the Ir remains near the surface following annealing, since we observe a proportional increase in surface structures with an increase in Ir deposition. In Fig. 7, the first layer of Ir sits in 3-fold hollow sites on the unreconstructed Ge substrate. Directly above this is a layer of Ge nearly on top sites of the Ge bulk; the top sites are the expected binding sites for Ge. The positioning of the first layer of Ir in hollow sites provides sufficient room for Ge to bond with no change to the bond length, taking into account the Ir and Ge bulk radii. Ir is located in similar sites for a model of Ir/Si(100) [29]. The second layer of Ir is shown as trimers to reflect our observation of a $\sqrt{3}$ reconstruction of the islands. Similar trimers are proposed as the model for Au/Ge(111) [13, 31].

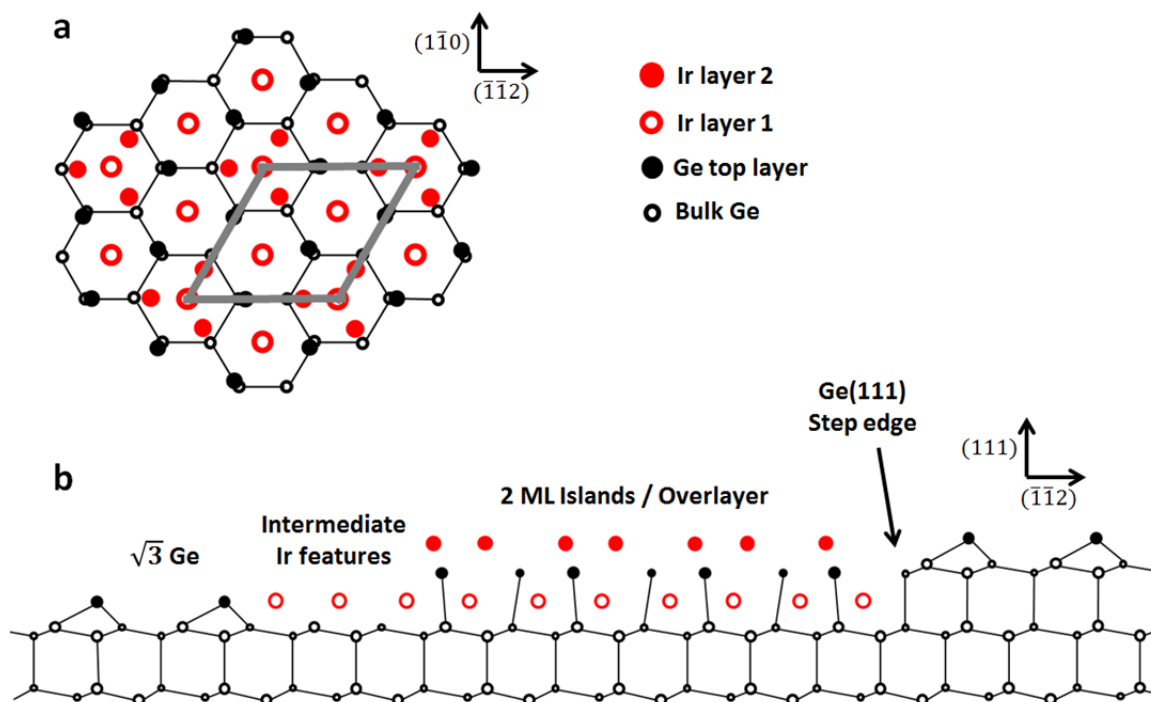


Figure 7: (a) Top view of a model for 2.0 ML Ir islands with the $\sqrt{3}$ unit-cell outlined. (b) Side view of the same model for Ir islands also showing intermediate features, a $\sqrt{3}$ Ge substrate reconstruction, and a Ge step-edge.

In the formation of these islands, the first layer of Ir and the Ge top layer would have to form before the second layer of Ir. The locations of intermediate features, which have been observed to directly border 2.0 ML features, are consistent with this process. In the simplest case, pathways may correspond to a single layer of Ir adsorption as presented in Fig. 7.

According to this model, the islands/overlayer would require 1.0 ML of Ge atoms. The original $c(2\times 8)$ Ge reconstruction consists of 0.25 ML Ge adatoms, and a complete surface reconstruction to $\sqrt{3}$ would require 0.33 ML Ge. The Ge substrate, though, contains a number of vacancies, and our model suggests that the locations of dots and pathways also correspond to locations without Ge adatoms. Considering diffusion from step edges, and our data which show numerous Ge adatom vacancies, we suspect that there may be sufficient Ge atoms to form 1.0 ML within the islands. Another possible model for the islands might include the formation of a double layer (2.0 ML) of Ge above the first layer of Ir; due to the large number of Ge atoms required, we do not suspect it is the case. Yet another possibility might include the formation of the second layer of Ir directly on top of the first layer Ir, with no Ge layer in the island structure; but due to the alloying tendency of semiconductors and transition metals, we do not include this option.[12, 29, 30, 32]

4. Conclusions

Island formation of the Ir/Ge(111) surface was studied using UHV STM. An increase in Ir coverage correlates with an increase in island coverage, and a complete overlayer is formed with 2.0 ML of Ir. Annealing samples to temperatures above 600 K results in the formation of tall

islands. For annealing temperatures above 650 K, these islands become more round, and features of an intermediate height are observed which we have described as pathways and dots.

Annealing temperatures above 650 K also cause a $\sqrt{3}$ reconstruction of both the substrate and the islands. The pathways form along the antiphase domain boundaries between competing surface domains of the Ge surface reconstruction, and also along the upper step-edges of the Ge substrate. Islands form at locations where domain boundaries intersect; this gives the appearance of the Ir in the domain boundaries forming pathways between different islands. All the features that we associate with Ir adsorption change similarly in apparent height with a change in the tip state (Fig. 3). The islands formed from higher annealing temperatures resulted in larger island sizes, which is evidence of Ostwald ripening.

Our model for the islands/overlayer accounts for 2.0 ML of Ir and assumes the diffusion of 1.0 ML Ge into the structure. The intermediate features are modeled as locations with 1.0 ML Ir adsorption. The model accounts for the $\sqrt{3}$ reconstruction with trimers of Ir on the top-most layer.

Acknowledgments

The authors are pleased to acknowledge funding support from the National Science Foundation under Grants CHE-0719504 and PHY-1004848.

References

- [1] C. H. Mullet and S. Chiang, *Surf. Sci.* 621, (2014) 184.
- [2] Y. Sato, S. Chiang, and N. C. Bartelt, *Phys. Rev. Lett.* 99, (2007) 096103.
- [3] Y. Sato and S. Chiang, *Surf. Sci.* 603, (2009) 2300.
- [4] J. A. Giacomo, Ph.D. dissertation in Physics, University of California, Davis, California (2009).
- [5] C. H. Mullet, Ph.D. dissertation in Physics, University of California, Davis, California (2012).
- [6] C. H. Mullet and S. Chiang, *Journal of Vacuum Science & Technology A* 31, (2013) 020602.
- [7] B. H. Stenger, A. L. Dorsett, J. H. Miller, E. M. Russell, C. A. Gabris, and S. Chiang, *Ultramicroscopy* in press, (2017) <http://dx.doi.org/10.1016/j.ultramic.2017.05.005>.
- [8] C. H. Mullet, B. H. Stenger, A. M. Durand, J. A. Morad, Y. Sato, E. C. Poppenheimer, and S. Chiang, manuscript submitted to *Surface Science*, (2017).
- [9] Ernst Bauer, *Zeitschrift für Kristallographie-Crystalline Materials* 110, (1958) 372.
- [10] Oguzhan Gurlu, Omer A. O. Adam, Harold J. W. Zandvliet, and Bene Poelsema, *Applied Physics Letters* 83, (2003) 4610.
- [11] Carl Wagner, *Zeitschrift für Elektrochemie, Berichte der Bunsengesellschaft für physikalische Chemie* 65, (1961) 581.
- [12] A. Wawro, S. Suto, and A. Kasuya, *Phys. Rev. B* 72, (2005) 205302.
- [13] L. Seehofer and R. L. Johnson, *Surf. Sci.* 318, (1994) 21.
- [14] Y. G. Ding, C. T. Chan, and K. M. Ho, *Phys. Rev. Lett.* 67, (1991) 1454.
- [15] W. Telieps and E. Bauer, *Ultramicroscopy* 17, (1985) 57.
- [16] W. Telieps and E. Bauer, *Surf. Sci.* 200, (1988) 512.
- [17] G. Binnig, H. Rohrer, Ch Gerber, and E. Weibel, *Phys. Rev. Lett.* 49, (1982) 57.
- [18] C. L. H. Devlin, D. N. Futaba, A. Loui, J. D. Shine, and S. Chiang, *Mat Sci Eng B-Solid* 96, (2002) 215.
- [19] D. J. Chadi and C. Chiang, *Physical Review B* 23, (1981) 1843.
- [20] I. Razado-Colambo, Jiangping He, H. M. Zhang, G. V. Hansson, and R. I. G. Uhrberg, *Physical Review B* 79, (2009) 205410.
- [21] I. Horcas, R. Fernández, J. M. Gómez-Rodríguez, J. Colchero, J. Gómez-Herrero, and A. M. Baro, *Review of Scientific Instruments* 78, (2007) 013705.
- [22] Werner Smekal, Wolfgang S. M. Werner, and Cedric J. Powell, *Surface and Interface Analysis* 37, (2005) 1059.
- [23] W. C. Fan and A. Ignatiev, *Phys. Rev. B* 40, (1989) 5479.
- [24] J. Nogami, A. A. Baski, and C. F. Quate, *Phys. Rev. Lett.* 65, (1990) 1611.
- [25] M. M. R. Evans, J. C. Glueckstein, and J. Nogami, *Physical Review B* 53, (1996) 4000.
- [26] Robert D. Meade and David Vanderbilt, *Physical Review B* 40, (1989) 3905.
- [27] W. C. Fan, A. Ignatiev, H. Huang, and S. Y. Tong, *Phys. Rev. Lett.* 62, (1989) 1516.
- [28] R. M. Feenstra and G. A. Held, *Physica D: Nonlinear Phenomena* 66, (1993) 43.
- [29] Ute Hörmann, Thilo Remmele, John E. Klepeis, Oleg Pankratov, Holger Grünleitner, Max Schulz, Meiken Falke, and Andrew Bleloch, *Physical Review B* 79, (2009) 104116.
- [30] A. Habanyama and C. M. Comrie, *Thin Solid Films* 516, (2008) 5137.
- [31] P. B. Howes, C. Norris, M. S. Finney, E. Vlieg, and R. G. van Silfhout, *Physical Review B* 48, (1993) 1632.
- [32] J. G. White and E. F. Hockings, *Inorganic Chemistry* 10, (1971) 1934.